RESEARCH PAPER

Organogenesis 9:3, 161–167; July/August/September 2013; © 2013 Landes Bioscience

Heparinized collagen scaffolds with and without growth factors for the repair of diaphragmatic hernia

Construction and in vivo evaluation

Katrien M Brouwer,[1] René M Wijnen,[2,†] Daphne Reijnen,[3] Theo G Hafmans,[1] Willeke F Daamen[1] and Toin H van Kuppevelt[1,*]

[1]Department of Biochemistry; NCMLS; Radboud University Nijmegen Medical Centre; Nijmegen, The Netherlands; [2]Department of Surgery; Radboud University Nijmegen Medical Centre; Nijmegen, The Netherlands; [3]Central Animal Facility; Radboud University Nijmegen Medical Centre; Nijmegen, The Netherlands

[†]Current affiliation: Department of Pediatric Surgery; Erasmus MC Sophia Children's Hospital; Rotterdam, The Netherlands

Keywords: collagen, diaphragm, growth factors, heparin, regenerative medicine, scaffold, vascularization

Abbreviations: DAB, 3,3'-diaminobenzidine; EDC, 1-ethyl-3-(3-dimethylaminopropyl)carbodiimide; Hep, heparin; HGF, hepatocyte growth factor; MES, 2-morpholinoethanesulfonic acid; NHS, N-hydroxysuccinimide; PBS, phosphate buffered saline; PTFE, polytetrafluoroethylene; SDS-PAGE, sodium dodecyl sulphate polyacrylamide gel electrophoresis; SEM, scanning electron microscopy; SIS, small intestinal submucosa; VEGF, vascular endothelial growth factor; X, crosslinked

A regenerative medicine approach to restore the morphology and function of the diaphragm in congenital diaphragmatic hernia is especially challenging because of the position and flat nature of this organ, allowing cell ingrowth primarily from the perimeter. Use of porous collagen scaffolds for the closure of surgically created diaphragmatic defects in rats has been shown feasible, but better ingrowth of cells, specifically blood vessels and muscle cells, is warranted. To stimulate this process, heparin, a glycosaminoglycan involved in growth factor binding, was covalently bound to porous collagenous scaffolds (14%), with or without vascular endothelial growth factor (VEGF; 0.4 μg/mg scaffold), hepatocyte growth factor (HGF; 0.5 μg/mg scaffold) or a combination of VEGF + HGF (0.2 + 0.5 μg/mg scaffold). All components were located primarily at the outside of scaffolds. Scaffolds were implanted in the diaphragm of rats and evaluated after 2 and 12 weeks. No herniations or eventrations were observed, and in several cases, growth factor-substituted scaffolds showed macroscopically visible blood vessels at the lung site. The addition of heparin led to an accelerated ingrowth of blood vessels at 2 weeks. In all scaffold types, giant cells and immune cells were present primarily at the liver side of the scaffold, and immune cells and individual macrophages at the lung side; these cell types decreased in number from week 2 to week 12. The addition of growth factors did not influence cellular response to the scaffolds, indicating that further optimization with respect to dosage and release profile is needed.

Introduction

Diaphragmatic defects in children with congenital diaphragmatic hernia are closed by primary repair in the case of smaller defects, but a patch is needed for repair in larger defects. Patch materials commonly applied include polytetrafluoroethylene (PTFE)[1] and small intestinal submucosa (SIS), derived from decellularised porcine submucosa.[2] Both types of materials have been found successful in some studies,[3-5] but showed high recurrence rates in others.[2,6,7] A recent meta-analysis reported no differences between PTFE and SIS, both materials having a recurrence rate of over 30%.[7] In case of PTFE patches this may be due to the lack of growth of the material with the child[8] and limited cellular infiltration.[9] With regard to cellular ingrowth the diaphragm may be especially challenging. Due to its flat nature, cellular migration from the periphery of diaphragm into the central part of the scaffolds will primarily occur from the side, limiting the surface over which ingrowth can occur. For SIS, a degradable biological material that may be substituted by the patient's own tissue and thus has the ability to grow with the child, it has been suggested that additional perforation of the material may enhance vascularization.[2] Moreover, it has been suggested that SIS is degraded too fast as the manufacturer indicated resorption of the material in 2 weeks.[7] In a previous study,[10] we have therefore used porous type I collagen bioscaffolds, strengthened by crosslinking, to close surgically created diaphragmatic defects in rats. Scaffold degradation and deposition of new collagen and of mesothelium were observed, and reherniations did not occur.

*Correspondence to: Toin H van Kuppevelt; Email: A.vanKuppevelt@ncmls.ru.nl
Submitted: 04/05/13; Revised: 06/13/13; Accepted: 06/28/13
http://dx.doi.org/10.4161/org.25587

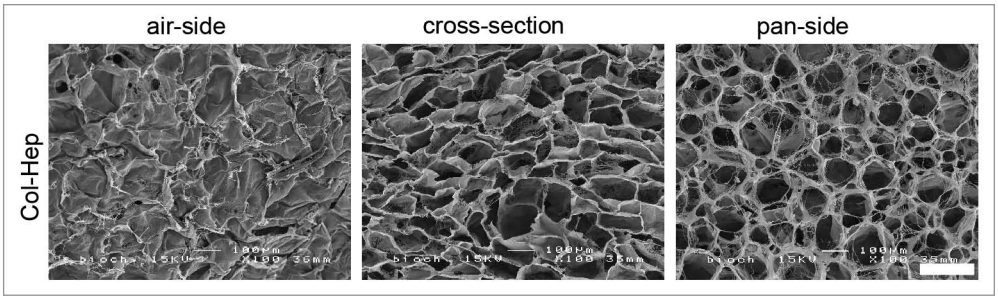

Figure 1. Morphology of porous collagen scaffolds crosslinked with heparin (Col-Hep) (scanning electron microscopical images). Air-side and pan-side represent the side exposed to the air or to the mold while producing the scaffold, respectively. Bar represents 200 μm.

Blood vessels were present at the outer borders of the scaffold, but were modest in number in the center of the scaffold. Muscle fibers and cells had infiltrated into the scaffold in some cases; however, muscle mostly grew over instead of into the scaffold, and only for a limited distance.

In this study, we aimed to stimulate muscle cell and blood vessel ingrowth by the addition of bioactive factors to the scaffold. Scaffolds were crosslinked in the presence of heparin, a polysaccharide capable of sequestering growth factors. Growth factors reported to stimulate muscle cells and/or blood vessels viz. hepatocyte growth factor (HGF) and vascular endothelial growth factor (VEGF), both heparin binding proteins,[11-14] were attached to the scaffold before implantation. Scaffolds were biochemically and morphologically characterized and implanted into a surgically created diaphragmatic hernia in rats to study degradation, cellular infiltration and tissue regeneration.

Results

Scaffold characteristics. Scaffolds showed a high porosity at cross sections, and a somewhat more closed surface on pan and especially air sides, as observed with scanning electron microscopy (SEM) (**Fig. 1**). Crosslinking efficiency was 36% ± 3% (mean ± standard error of the mean) for Col-X scaffolds and 46% ± 8% for Col-Hep scaffolds. Per mg Col-Hep scaffold, 139 ± 11 μg heparin (mean ± standard error of the mean) was bound; histology showed that heparin was localized mostly at the outer borders of the scaffold (**Fig. 2**). The amount of growth factor bound to the scaffolds was 0.2 and 0.4 μg VEGF/mg scaffold, for Col-Hep-VH and Col-Hep-V scaffolds, respectively, and 0.5 μg HGF/mg scaffold for both Col-Hep-VH and Col-Hep-H scaffolds (**Fig. 2**). Growth factors were mostly localized at the outer borders of the scaffolds, as was heparin (**Fig. 2**).

General appearance and macroscopic evaluation. Survival of the rats was 100%. Rats recovered well after surgery, wound healing was normal and no further pain medication was administered beyond two days after surgery. Rats were sacrificed at 2 or 12 weeks after the operation. Scaffolds did not show any signs of mechanical weakness, nor were diaphragmatic eventrations or herniations observed. Scaffolds were easily recognized by their whitish appearance and the non-absorbable sutures were also visible. The absorbable sutures were well visible at week 2 and after 12 weeks stitch marks from these sutures were sometimes still visible.

At two weeks, Col-X and Col-Hep scaffolds were comparable in their macroscopical appearance, with a distinctly demarcated boundary between scaffold and diaphragm. This boundary was less clear for scaffolds with growth factors where a more faded border between scaffold and diaphragm was present. On the lung side of 2 out of 4 of the Col-Hep-V and Col-Hep-VH scaffolds, blood vessels were visible macroscopically on the outer edges of the scaffolds; this was not observed for any of the other scaffolds at two weeks after implantation.

At 12 weeks, scaffolds remained whitish. Blood vessels were observed on the outer edges of the lung sides for some Col-Hep-V, Col-Hep-H and Col-Hep-VH scaffolds (**Fig. 3**), but not for Col-X and Col-Hep scaffolds. Adhesions between the scaffold and the liver were present in all animals; adherence to the lungs was never observed.

Microscopic examination. A systematic survey using five different types of scaffolds allowed us to evaluate the contribution of the different components. Cellular response to the scaffold was scored (summarized in **Table 1**). A number of cell types were scored including mast cells, phagocytes (macrophages and giant cells) and immune cells (lymphocytes, plasma cells and polymorphonuclear leucocytes). Cellular response varied between the animals in each group. The most important findings are described below. Results for CD68, desmin and α smooth muscle actin staining are not shown, as no differences between the different groups could be observed.

Two weeks after implantation. At two weeks after implantation, blood vessels were predominantly present at the liver side of the scaffold and at the border between scaffold and original diaphragm in all scaffolds. At these places in the scaffolds, also most cells were present. Col-Hep scaffolds showed the largest amount of blood vessels, significant against Col-Hep-V and Col-Hep-VH ($p < 0.05$) (**Fig. 4**). No statistical significant differences between the other scaffold types were observed. Blood vessels were functional since erythrocytes were observed inside the vessel lumina. With respect to the effect of the scaffolds on muscle tissue, the growth of muscle on top of the scaffold was most often observed be it to a limited extent. Some ingrowth, however, was also observed. No clear differences between scaffold types were observed.

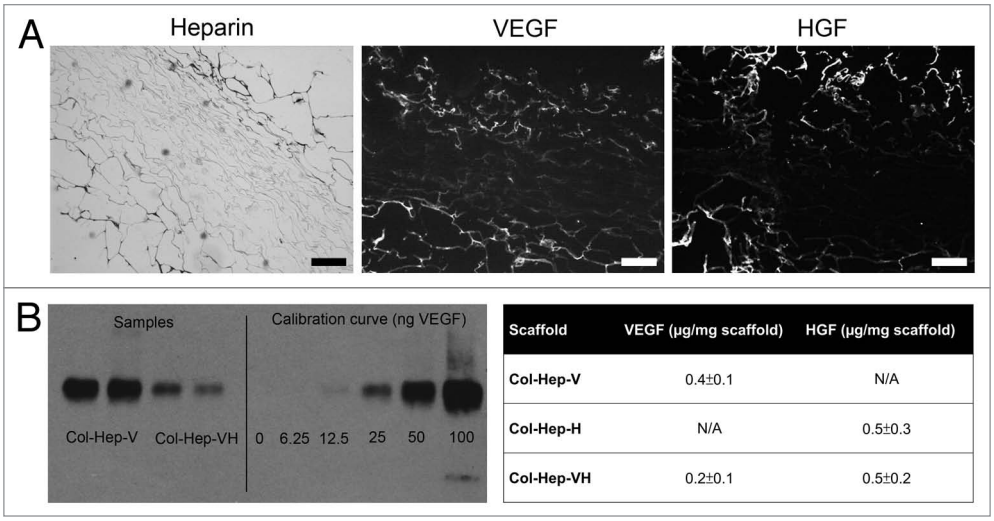

Scaffold	VEGF (µg/mg scaffold)	HGF (µg/mg scaffold)
Col-Hep-V	0.4±0.1	N/A
Col-Hep-H	N/A	0.5±0.3
Col-Hep-VH	0.2±0.1	0.5±0.2

Figure 2. Immunolocalization of heparin and growth factors, and quantification of growth factors. (**A**) Heparin and growth factors were primarily located at the outer sites of the scaffolds, as evidenced by toluidin blue (heparin) and immunofluorescent staining (VEGF, HGF) of a Col-Hep scaffold and a Col-Hep-VH scaffold. Bars represent 200 µm. (**B**) Western blot for VEGF bound to Col-Hep-V and Col-Hep-VH scaffolds, and table indicating the amount of growth factors bound to scaffolds. Values depicted as mean of three experiments ± standard deviation. N/A, not applicable; Hep, heparin; V, VEGF; H, HGF.

Cells penetrated into the scaffold only to a limited extent and sparse cells were present in the centers of the scaffolds for all scaffold types. No major differences between scaffold types were observed. At the liver side of the scaffolds, a layer of newly deposited collagen was present, as well as immune cells, phagocytes and giant cells. The extent of immune cell influx and the amount of phagocytes was similar between the different scaffold types. At the lung side of the scaffolds, a layer of newly deposited collagen could be observed occasionally. In total, the amount of phagocytes and immune cells (in the entire scaffold) was comparable for the different scaffold types.

Twelve weeks after implantation. At 12 weeks after implantation, the amount of blood vessels was comparable to that of week 2 (**Fig. 4**), be it that the blood vessels were distributed somewhat more into the scaffold centers in part of the scaffolds. The differences in the amount of blood vessels between Col-Hep scaffolds and Col-Hep-V and Col-Hep-VH at week 2 were not present at 12 weeks after implantation, indicating an accelerated angiogenesis at an early point in time for the Col-Hep scaffolds. As at 2 weeks after implantation, overgrowth of muscle was typically observed, with some ingrowth.

Scaffold centers still remained relatively free of cells although blood vessels had infiltrated somewhat further into the scaffolds. The amount of cells in the center was similar to those at week 2 for all scaffolds. Generally, immune cells and phagocytes decreased in number from week 2 to week 12 after implantation (although not always statistically significant), immune cells were observed mostly at the liver side of the scaffold as well as the border between scaffold and original diaphragm. Phagocytes were located primarily at the liver side, whereas giant cells were mostly observed at the border between scaffold and original diaphragm. At the lung side immune cells and individual macrophages were observed. As at 2 weeks after implantation, a layer of newly deposited collagen was occasionally seen at the lung side of the scaffold, somewhat thicker than at 2 weeks after implantation. Mast cells remained present, mainly at the lung side of the scaffold.

Discussion

New biological materials to be used in closure of diaphragmatic defects are currently investigated. The use of porous collagen scaffolds has previously been shown feasible in a rat model for diaphragmatic hernia,[10] but muscle cell and blood vessel ingrowth were limited. Therefore, collagen scaffolds with heparin, HGF and VEGF were produced. Heparin is able to sequester a large number of angiogenic factors, and when attached to collagen it may lead to an increase of endothelial cell proliferation.[15] In this study, heparin was covalently attached to collagen scaffolds using EDC/NHS crosslinking, and, although located primarily at the outside of the scaffolds, at 2 weeks after implantation in rat diaphragm significant differences were found for the amount of blood vessels in Col-Hep compared with two other scaffold types, which is indicative that heparin induced blood vessel formation. Blood vessels were generally functional as red blood cells were observed in the lumens. The presence of blood vessels might render hypoxia in the scaffold less likely, thereby stimulating cell survival and tissue replacement.

Other stimulatory molecules added to the scaffolds in this study were VEGF and HGF. VEGF is a regulator of angiogenesis,[16] and an increase in angiogenic potential of collagen-heparin scaffolds by addition of VEGF,[15] has been observed. VEGF and FGF2 attached to Col-Hep scaffolds increased the amount and the maturity of blood vessels.[17] VEGF stimulates endothelial cells by binding to VEGFR-2, heparin/heparan sulfate being a co-receptor, and induces matrix metalloproteinase (MMP)

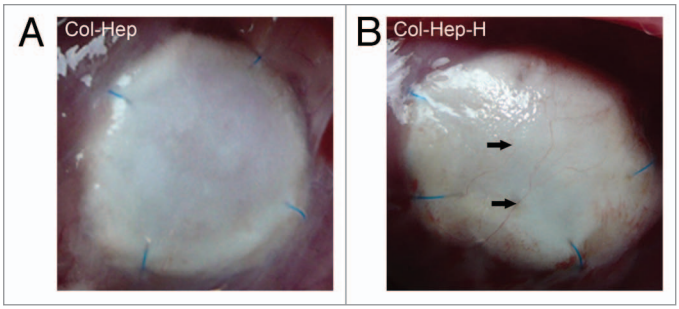

Figure 3. Macroscopical view of Col-Hep (**A**) and Col-Hep-H (**B**) scaffolds at 12 weeks after implantation. Arrows point at blood vessels at the lung side of Col-Hep-H scaffolds, which were not observed on Col-Hep scaffolds. Blue lines are non-absorbable sutures. Hep, heparin; H, HGF.

production, proliferation and migration.[17] Moreover, VEGF attracts macrophages, which in turn produce VEGF as well as MMPs that release additional VEGF from the surrounding tissue.[18,19] HGF is also an angiogenic agent, and the combination with VEGF is potent,[20] as HGF enhances VEGF-induced angiogenesis both in vitro and in vivo.[13,21] Combined treatment with HGF and VEGF could therefore be superior to treatment with either one factor by enhancing angiogenesis while avoiding inflammation.[14] Besides stimulating angiogenesis, HGF is known for its stimulation of skeletal muscle cell/satellite cell activation, proliferation and differentiation.[11,12,22] Although we observed in this study blood vessels at the lung side of growth factor loaded scaffolds, we did not observe statistically significant cellular effects of VEGF and/or HGF inside the scaffolds. In another study on diaphragm repair, VEGF-loaded porous silica gel (with or without myoblasts) on acellular diaphragmatic matrix led to increased vascularity but also increased inflammatory response, contraction and fibrotic tissue. The authors argued that this could be due to an abnormal angiogenic response following a high local growth factor concentration.[23] Growth factor amounts were lower in their experiment, as they loaded 200 ng VEGF/implant compared with 0.2/0.4 μg/mg scaffold in our study (we on average used scaffolds of 8 mg). However, release may differ between silica gels and the heparin-bound growth factors in our study.

The limited response to the growth factors on our scaffolds may have been caused by the organ system studied, as ingrowth of cells in this diaphragm model was primarily possible from the sides of the scaffold, limiting the surface area available for ingrowth. Thus the contact area may have been considerable less in comparison to e.g., subcutaneously implanted scaffolds, where response to growth factors has been observed.[17,24] An increased cellular reaction may be necessary to trigger angiogenesis.[25] Moreover, heparin and growth factors were located primarily at the outside of the scaffolds, and this may have limited cellular ingrowth into the central area. An improved scaffold design, in which heparin and growth factors are distributed throughout the scaffolds, may enhance the influx of cells into the scaffolds center. This may be accomplished e.g., by addition of heparin to the scaffold suspension before the freezing/lyophilization procedure.

In conclusion, the formation of blood vessels in collagen scaffolds for repair of diaphragmatic hernia was accelerated by the addition of heparin. The addition of growth factors did not lead to significant differences inside the scaffolds, possibly due to suboptimal release profiles and dose in combination with the model used. Additional research to controlled release of growth factors is needed.

Materials and Methods

This study was approved by the Ethical Committee on Animal research of the Radboud University Nijmegen Medical Centre under protocol number 2009–155.

Preparation of collagen bioscaffolds. Bioscaffolds were prepared using type I collagen fibrils derived from bovine Achilles' tendon,[26] as previously described.[27,28] A 0.8% (w/v) suspension of insoluble type I collagen in 0.25 M acetic acid was prepared. The suspension was then poured into 12-wells plates (1.6 ml/well), frozen for at least 4 h at –20°C and lyophilized in a Zirbus lyophiliser. Resulting porous scaffolds were chemically crosslinked using 1-ethyl-3-(3-dimethylaminopropyl)carbodiimide (EDC) and N-hydroxysuccinimide (NHS). For this, collagen scaffolds were incubated for 30 min in 50 mM 2-morpholinoethanesulphonic acid (MES) (pH 5.0) containing 40% (v/v) ethanol and crosslinked by immersion for 4 h at room temperature in 4 ml 33 mM EDC, 6 mM NHS in 50 mM MES (pH 5.0) containing 40% ethanol, in the presence or absence of 0.25% heparin (Diosynth, 41050.2). The scaffolds were then washed in 0.1 M Na_2HPO_4, 1 M NaCl, 2 M NaCl and demineralized water, and stored in 70% ethanol at –20°C.

Before implantation, the scaffolds were disinfected in 70% ethanol for a total duration of 22 h (5 × 2.8 ml per well) and washed with sterile phosphate buffered saline (PBS) (9 × 2.8 ml per well), for a total duration of 22 h also.

The growth factors vascular endothelial growth factor (recombinant rat VEGF 164, produced in our laboratory[29]) and hepatocyte growth factor (recombinant mouse HGF, R&D Systems, 2207-HG/CF) were loaded onto the heparin containing collagen scaffolds. For scaffolds containing one growth factor, scaffolds were incubated overnight in 2 ml PBS containing 10 μg/ml VEGF or 10 μg/ml HGF. Scaffolds containing both VEGF and HGF were first incubated for 1 h in a PBS solution containing VEGF, after which HGF was added for an overnight incubation. The end concentration of both growth factors was 5 μg/ml. All scaffolds were washed for 3 times 15 min with 2 ml PBS before implantation.

The following abbreviations for scaffolds were used: Col-X: crosslinked collagen scaffold, Col-Hep: crosslinked scaffolds with heparin, Col-Hep-V: crosslinked scaffolds with heparin and VEGF, Col-Hep-H: crosslinked scaffolds with heparin and HGF, and Col-Hep-VH: crosslinked scaffolds with heparin, VEGF+HGF.

Analysis of collagen scaffolds. Morphology of the scaffolds was visualized by SEM. Wet scaffolds were dehydrated to 100%

Table 1. Cells present in scaffolds at 2 and 12 weeks

Scaffold	Time after implantation	Cells in scaffold center	Blood vessels[A]	Muscle ingrowth	Muscle overgrowth	Mast cells total[a]	Phagocytes[b]	Immune cells[c]
Col-X	2 weeks	1.0 ± 0.0	1.0 ± 0.0	0.5 ± 0.7	1.0 ± 1.4	1.5 ± 0.7	1.3 ± 0.4	1.3 ± 0.4
	12 weeks	1.0 ± 0.0	1.0 ± 0.0	0.3 ± 0.4	0.0 ± 0.0	1.0 ± 0.0	0.8 ± 0.4	0.5 ± 0.0
Col-Hep	2 weeks	1.0 ± 0.0	1.9 ± 0.3[B,C]	0.0 ± 0.0	0.8 ± 1.0	1.6 ± 0.5	2.3 ± 0.3	2.1 ± 0.5
	12 weeks	1.5 ± 0.7	1.6 ± 0.9	0.3 ± 0.3	0.5 ± 0.4	2.1 ± 0.9	1.4 ± 0.8	1.5 ± 0.7
Col-Hep-V	2 weeks	1.3 ± 0.3	1.0 ± 0.0[B]	0.0 ± 0.0	1.0 ± 0.7	1.0 ± 0.0	1.8 ± 0.3	1.9 ± 0.5
	12 weeks	1.0 ± 0.4	1.7 ± 0.6	1.3 ± 0.8	1.7 ± 1.2	2.3 ± 1.0	0.8 ± 0.3	0.6 ± 0.3
Col-Hep-H	2 weeks	1.3 ± 0.3	1.6 ± 0.5	0.1 ± 0.3	0.9 ± 1.0	2.0 ± 1.2	1.8 ± 0.3	2.1 ± 0.6
	12 weeks	1.1 ± 0.5	1.3 ± 0.5	0.3 ± 0.4	0.5 ± 0.7	1.8 ± 0.3	0.6 ± 0.3	0.9 ± 0.3
Col-Hep-VH	2 weeks	1.1 ± 0.3	1.1 ± 0.3[C]	0.0 ± 0.0	1.1 ± 0.9	1.5 ± 0.4	2.0 ± 0.6	1.5 ± 0.4
	12 weeks	1.1 ± 0.3	1.3 ± 0.5	0.2 ± 0.3	0.6 ± 0.3	2.1 ± 0.9	0.9 ± 0.5	0.8 ± 0.5

Scoring for all parameters was performed on a scale from 0–3. [a]The absolute numbers for mast cells are much lower than for phagocytes and immune cells. [b]Phagocytes include giant cells and macrophages. [c]Immune cells exclude mast cells and phagocytes. [A]2-week groups differed with statistical significance according to Independent Samples Kruskal Wallis-test ($p < 0.05$). Statistically significant differences between two sets of groups were assessed using Independent Samples Mann-Whitney U-test for non-parametric data and are indicated by equal symbols for both groups. [B,C]$p < 0.05$. Parameters that differed with statistical significance between 2 and 12 weeks are shown underlined, as assessed using Independent Samples Mann-Whitney U-test for non-parametric data.

ethanol and critical point dried using liquid CO_2. Specimens were mounted on stubs, sputtered with an ultrathin layer of gold in a Polaron E5100 coating system (Quorum Technologies) and visualized with a JEOL JSM-6310 SEM apparatus (JEOL) operating at 15 kV.

The degree of crosslinking of the scaffolds was determined spectophotometrically by determining the amine group content using 2,4,6-trinitrobenzene sulphonic acid.[30,31] Crosslinking efficiency was expressed as the number of amine groups used in crosslinking as a percentage of the total number of amine groups available. The heparin content of the scaffolds was determined applying a hexosamine assay using p-dimethylamino-benzaldehyde, taking heparin as a standard.[32,33] The amount of growth factors bound to the scaffolds was determined with sodium dodecyl sulfate PAGE (SDS-PAGE) on 15% and 12% (w/v) gels, for VEGF and HGF, respectively, followed by western blotting with antibodies goat-anti-rat-VEGF (R&D Systems, AF-564), goat-anti-mouse HGF (R&D Systems, AF2207) and peroxidase conjugated rabbit-anti-goat IgG (H^+L) (Pierce, 31402). Collagen scaffolds with heparin were incubated with growth factors and the amount of growth factor bound was quantified using a calibration curve (0–100/0–200 ng of either VEGF or HGF), by incubation for 15 min in a boiling water bath in non-reducing sample buffer. The intensity of the bands on the blot was analyzed using Adobe Photoshop CS4 (Adobe) using inverted gray scale images to determine the amount of signal per band, and compared with the calibration curve.

The location of heparin on the scaffold was visualized using toluidin blue staining, and growth factors were visualized by immunofluorescence with anti-VEGF and anti-HGF antibodies, followed by Alexa-labeled secondary antibodies (see **Table 2** for antibodies and dilutions).

Animals. 36 male Wistar (WU) rats (Harlan Laboratories) of 230–250 g were caged in pairs in a controlled environment; food and water were available ad libitum. Rats were divided into groups of 2 or 4; follow-up after surgery was 2 or 12 weeks. Rats were implanted with different scaffolds: groups of 2 rats with Col-X and groups of 4 rats with Col-Hep, Col-Hep-V, Col-Hep-H, or Col-Hep-VH.

Table 2. Antibodies and dilutions

Antigen	Antibody	Dilution
Mouse-anti-CD68	MCA341R, AbD Serotec, Germany	1:500
Mouse-anti-Desmin	Desmin 33, Biogenex, USA	1:200
Rabbit-anti-Laminin	L9393, Sigma, USA	1:50
Mouse-anti-Alpha smooth muscle actin	Clone 1A4, Sigma, USA	1:30,000
Biotinylated donkey-anti-rabbit IgG	711–065–152, Jackson ImmunoResearch, UK	1:200
Biotinylated horse-anti-mouse IgG	Vectastain ABC Kit mouse IgG, CA, USA	1:200
Alexa 488-labeled donkey-anti-goat IgG	A-11055, Molecular Probes, UK	1:200

Surgical procedure. Surgery was performed as described previously.[10] In short, a right-sided diaphragmatic defect of approximately 12 mm in diameter was created, and a scaffold was implanted with an overlap of scaffold with respect to the diaphragm at the abdominal side. Four non-absorbable interrupted sutures (Prolene 6–0) and 2–5 absorbable interrupted sutures (Vicryl 5–0, Ethicon) were used around the perimeter of the scaffold to close the defect.

Explantation of the diaphragms. Rats were sacrificed at the designated time points after surgery (2 or 12 weeks) by exposure to carbogen followed by carbon dioxide asphyxiation. Scaffold implantation sites could be identified by the non-absorbable sutures used at implantation of the scaffolds, and by their whitish color. Tissue was resected approximately 2 mm from the edge of the implant. Liver that adhered to the implant was not removed, and therefore also fixed and embedded. Half the implant was

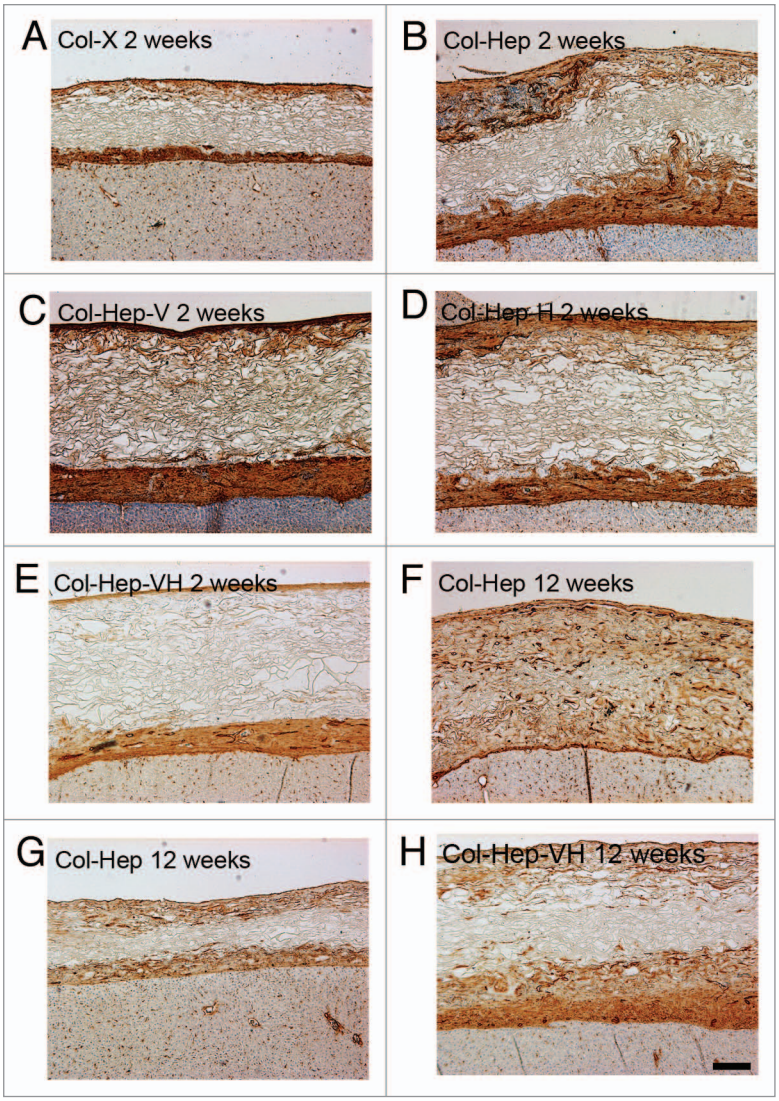

Figure 4. Vascularization of scaffolds (laminin staining). At two weeks, the scaffold substituted with heparin (Col-Hep; **B**) contained more blood vessels than other scaffolds (**A and C–E**). No significant differences between scaffolds types were observed at 12 weeks after implantation (**F–H**), although some variation between scaffolds was visible in distribution of blood vessels, both between and within groups. Bar represents 200 μm. Hep, heparin; V, VEGF; H, HGF.

fixed in formaldehyde and paraffin embedded; the other half was placed in optimal cutting temperature compound (Tissue-Tek, Sakura, 4583) and snap frozen in 2-methylbutane cooled with liquid nitrogen. The corresponding part of the left side of the diaphragm was resected to serve as control tissue and was processed likewise.

Immunohistological analysis. Paraffin embedded specimens were sectioned (5 μm) such as to include edge and center of the implants. Sections were mounted on Superfrost Plus glass slides, dried overnight at 37°C, and stained with hematoxylin and eosin[34] and Elastic Verhoeff Masson stain.[35]

Paraffin sections were also used to stain for desmin, and α smooth muscle actin by the following protocol. Sections were deparaffinated and rehydrated, after which antigen retrieval was performed by microwave exposure for 10 min in 10 mM citrate buffer (pH 6.0). Slides were allowed to cool down for at least 90 min. Endogenous peroxidase was blocked by incubation in 3% (v/v) hydrogen peroxide in PBS for 30 min. Subsequently, blocking with 5% serum in PBS-1% (w/v) BSA (bovine serum albumin) was performed, after which sections were incubated with the first antibody overnight at 4°C (see **Table 2** for antibodies and dilutions). Sections were then incubated with a biotinylated secondary antibody at 1:200 dilution, followed by the avidin-biotin-peroxidase complex (Vector Laboratories) and developed by incubation with 3,3'-diaminobenzidine (DAB), with hematoxylin counterstaining. For negative controls, the primary antibody was omitted.

CD68 staining on paraffin sections was performed by deparaffination and rehydration, after which antigen retrieval was performed by incubation in 10 mM citrate buffer (pH 6.0) at room temperature for 120 min. Further staining was performed as described.

Laminin staining on paraffin sections was performed by deparaffination, rehydration and subsequent incubation for 30 min in 0.1% (w/v) pronase in PBS at 37°C. Endogenous peroxidase was blocked using 0.3% (v/v) hydrogen peroxide in PBS for 30 min; further staining was performed as described.

Scoring. Two observers evaluated the staining results (KB, WD). Where differences occurred, slides were re-evaluated by the two observers together and consensus was obtained. Scoring was performed using a scale from 0 (absent) to 3 (abundantly present).

Statistical analysis. Statistical significance was determined using Independent Samples Kruskal Wallis-test for comparisons between scaffolds, and differences between two sets of groups were assessed using Independent Samples Mann-Whitney U-test for non-parametric data (SPSS statistical software package [version 19.0]). Differences were considered statistically significant at $p \leq 0.05$.

Disclosure of Potential Conflicts of Interest

No potential conflicts of interest were disclosed.

Acknowledgments

Etienne van Bracht, Arie Oosterhof and Elly Versteeg are kindly acknowledged for their technical assistance. This work was financially supported by EU-FP6 project EuroSTEC (soft tissue engineering for congenital birth defects in children: contract: LSHB-CT-2006-037409).

References

1. Clark RH, Hardin WD Jr., Hirschl RB, Jaksic T, Lally KP, Langham MR Jr., et al. Current surgical management of congenital diaphragmatic hernia: a report from the Congenital Diaphragmatic Hernia Study Group. J Pediatr Surg 1998; 33:1004-9; PMID:9694085; http://dx.doi.org/10.1016/S0022-3468(98)90522-X
2. Grethel EJ, Cortes RA, Wagner AJ, Clifton MS, Lee H, Farmer DL, et al. Prosthetic patches for congenital diaphragmatic hernia repair: Surgisis vs. Gore-Tex. J Pediatr Surg 2006; 41:29-33, discussion 29-33; PMID:16410103; http://dx.doi.org/10.1016/j.jpedsurg.2005.10.005
3. de Kort LM, Bax KM. Prosthetic patches used to close congenital diaphragmatic defects behave well: a long-term follow-up study. Eur J Pediatr Surg 1996; 6:136-8; PMID:8817203; http://dx.doi.org/10.1055/s-2008-1066490
4. Riehle KJ, Magnuson DK, Waldhausen JH. Low recurrence rate after Gore-Tex/Marlex composite patch repair for posterolateral congenital diaphragmatic hernia. J Pediatr Surg 2007; 42:1841-4; PMID:18022433; http://dx.doi.org/10.1016/j.jpedsurg.2007.07.009
5. Tsai J, Sulkowski J, Adzick NS, Hedrick HL, Flake AW. Patch repair for congenital diaphragmatic hernia: is it really a problem? J Pediatr Surg 2012; 47:637-41; PMID:22498374; http://dx.doi.org/10.1016/j.jpedsurg.2011.11.054
6. Moss RL, Chen CM, Harrison MR. Prosthetic patch durability in congenital diaphragmatic hernia: a long-term follow-up study. J Pediatr Surg 2001; 36:152-4; PMID:11150455; http://dx.doi.org/10.1053/jpsu.2001.20037
7. Romao RLP, Nasr A, Chiu PPL, Langer JC. What is the best prosthetic material for patch repair of congenital diaphragmatic hernia? Comparison and meta-analysis of porcine small intestinal submucosa and polytetrafluoroethylene. J Pediatr Surg 2012; 47:1496-500; PMID:22901906; http://dx.doi.org/10.1016/j.jpedsurg.2012.01.009
8. Fauza DO, Marler JJ, Koka R, Forse RA, Mayer JE, Vacanti JP. Fetal tissue engineering: diaphragmatic replacement. J Pediatr Surg 2001; 36:146-51; PMID:11150454; http://dx.doi.org/10.1053/jpsu.2001.20034
9. Kimber CP, Dunkley MP, Haddock G, Robertson L, Carey FA, Cuschieri A. Patch incorporation in diaphragmatic hernia. J Pediatr Surg 2000; 35:120-3; PMID:10646788; http://dx.doi.org/10.1016/S0022-3468(00)80027-5
10. Brouwer KM, Daamen WF, Reijnen D, Verstegen RH, Lammers G, Hafmans TG, et al. Repair of surgically created diaphragmatic defect in rat with use of a cross-linked porous collagen scaffold. J Tissue Eng Regen Med 2013; 7:552-61; PMID:22589175.
11. Allen RE, Sheehan SM, Taylor RG, Kendall TL, Rice GM. Hepatocyte growth factor activates quiescent skeletal muscle satellite cells in vitro. J Cell Physiol 1995; 165:307-12; PMID:7593208; http://dx.doi.org/10.1002/jcp.1041650211
12. Tatsumi R, Anderson JE, Nevoret CJ, Halevy O, Allen RE. HGF/SF is present in normal adult skeletal muscle and is capable of activating satellite cells. Dev Biol 1998; 194:114-28; PMID:9473336; http://dx.doi.org/10.1006/dbio.1997.8803
13. Xin X, Yang S, Ingle G, Zlot C, Rangell L, Kowalski J, et al. Hepatocyte growth factor enhances vascular endothelial growth factor-induced angiogenesis in vitro and in vivo. Am J Pathol 2001; 158:1111-20; PMID:11238059; http://dx.doi.org/10.1016/S0002-9440(10)64058-8
14. Min JK, Lee YM, Kim JH, Kim YM, Kim SW, Lee SY, et al. Hepatocyte growth factor suppresses vascular endothelial growth factor-induced expression of endothelial ICAM-1 and VCAM-1 by inhibiting the nuclear factor-kappaB pathway. Circ Res 2005; 96:300-7; PMID:15637298; http://dx.doi.org/10.1161/01.RES.0000155330.07887.EE
15. Steffens GC, Yao C, Prével P, Markowicz M, Schenck P, Noah EM, et al. Modulation of angiogenic potential of collagen matrices by covalent incorporation of heparin and loading with vascular endothelial growth factor. Tissue Eng 2004; 10:1502-9; PMID:15588409
16. Ferrara N. Role of vascular endothelial growth factor in regulation of physiological angiogenesis. Am J Physiol Cell Physiol 2001; 280:C1358-66; PMID:11350730
17. Nillesen ST, Geutjes PJ, Wismans R, Schalkwijk J, Daamen WF, van Kuppevelt TH. Increased angiogenesis and blood vessel maturation in acellular collagen-heparin scaffolds containing both FGF2 and VEGF. Biomaterials 2007; 28:1123-31; PMID:17113636; http://dx.doi.org/10.1016/j.biomaterials.2006.10.029
18. Blau HM, Banfi A. The well-tempered vessel. Nat Med 2001; 7:532-4; PMID:11329048; http://dx.doi.org/10.1038/87850
19. Bergers G, Brekken R, McMahon G, Vu TH, Itoh T, Tamaki K, et al. Matrix metalloproteinase-9 triggers the angiogenic switch during carcinogenesis. Nat Cell Biol 2000; 2:737-44; PMID:11025665; http://dx.doi.org/10.1038/35036374
20. Van Belle E, Witzenbichler B, Chen D, Silver M, Chang L, Schwall R, et al. Potentiated angiogenic effect of scatter factor/hepatocyte growth factor via induction of vascular endothelial growth factor: the case for paracrine amplification of angiogenesis. Circulation 1998; 97:381-90; PMID:9468212; http://dx.doi.org/10.1161/01.CIR.97.4.381
21. Cimpean AM, Seclaman E, Ceaus-/u R, Gaje P, Feflea S, Anghel A, et al. VEGF-A/HGF induce Prox-1 expression in the chick embryo chorioallantoic membrane lymphatic vasculature. Clin Exp Med 2010; 10:169-72; PMID:20033752; http://dx.doi.org/10.1007/s10238-009-0085-6
22. Turner NJ, Badylak SF. Regeneration of skeletal muscle. Cell Tissue Res 2012; 347:759-74; PMID:21667167; http://dx.doi.org/10.1007/s00441-011-1185-7
23. Conconi MT, Bellini S, Teoli D, de Coppi P, Ribatti D, Nico B, et al. In vitro and in vivo evaluation of acellular diaphragmatic matrices seeded with muscle precursors cells and coated with VEGF silica gels to repair muscle defect of the diaphragm. J Biomed Mater Res A 2009; 89:304-16; PMID:18431788; http://dx.doi.org/10.1002/jbm.a.31982
24. Pieper JS, Hafmans T, van Wachem PB, van Luyn MJ, Brouwer LA, Veerkamp JH, et al. Loading of collagen-heparan sulfate matrices with bFGF promotes angiogenesis and tissue generation in rats. J Biomed Mater Res 2002; 62:185-94; PMID:12209938; http://dx.doi.org/10.1002/jbm.10267
25. van Amerongen MJ, Molema G, Plantinga J, Moorlag H, van Luyn MJ. Neovascularization and vascular markers in a foreign body reaction to subcutaneously implanted degradable biomaterial in mice. Angiogenesis 2002; 5:173-80; PMID:12831058; http://dx.doi.org/10.1023/A:1023822504224
26. Pieper JS, Oosterhof A, Dijkstra PJ, Veerkamp JH, van Kuppevelt TH. Preparation and characterization of porous crosslinked collagenous matrices containing bioavailable chondroitin sulphate. Biomaterials 1999; 20:847-58; PMID:10226711; http://dx.doi.org/10.1016/S0142-9612(98)00240-3
27. Hosper NA, Eggink AJ, Roelofs LA, Wijnen RM, van Luyn MJ, Bank RA, et al. Intra-uterine tissue engineering of full-thickness skin defects in a fetal sheep model. Biomaterials 2010; 31:3910-9; PMID:20170954; http://dx.doi.org/10.1016/j.biomaterials.2010.01.129
28. Faraj KA, van Kuppevelt TH, Daamen WF. Construction of collagen scaffolds that mimic the three-dimensional architecture of specific tissues. Tissue Eng 2007; 13:2387-94; PMID:17627479; http://dx.doi.org/10.1089/ten.2006.0320
29. Geutjes PJ, Nillesen ST, Lammers G, Daamen WF, van Kuppevelt TH. Cloning, large-scale production, and purification of active dimeric rat vascular endothelial growth factor (rrVEGF-164). Protein Expr Purif 2010; 69:76-82; PMID:19733244; http://dx.doi.org/10.1016/j.pep.2009.08.015
30. Gilbert DL, Kim SW. Macromolecular release from collagen monolithic devices. J Biomed Mater Res 1990; 24:1221-39; PMID:2211746; http://dx.doi.org/10.1002/jbm.820240907
31. Olde Damink LH, Dijkstra PJ, van Luyn MJ, van Wachem PB, Nieuwenhuis P, Feijen J. Cross-linking of dermal sheep collagen using a water-soluble carbodiimide. Biomaterials 1996; 17:765-73; PMID:8730960; http://dx.doi.org/10.1016/0142-9612(96)81413-X
32. Elson LA, Morgan WT. A colorimetric method for the determination of glucosamine and chondrosamine. Biochem J 1933; 27:1824-8; PMID:16745305
33. Yannas IV, Burke JF, Gordon PL, Huang C, Rubenstein RH. Design of an artificial skin. II. Control of chemical composition. J Biomed Mater Res 1980; 14:107-32; PMID:7358747; http://dx.doi.org/10.1002/jbm.820140203
34. Bancroft JD, Stevens A. Theory and Practice of Histological Techniques. Fourth edition ed. Churchill Livingstone 1996.
35. O'Connor WN, Valle S. A combination Verhoeff's elastic and Masson's trichrome stain for routine histology. Stain Technol 1982; 57:207-10; PMID:6183794